Supporting Information

Hierarchical Carbon@Ni_3S_2@MoS_2 Double Core-Shell Nanorods for High-Performance Supercapacitors

Laiquan Li[ab], Hongbin Yang[b], Liping Zhang[b], Jianwei Miao[b], Jun Yang[a], Yufei Zhang[a], ChenCheng Sun[a], Wei Huang[a], Xiaochen Dong*[a], and Bin Liu*[b]

[a]Key Laboratory of Flexible Electronics (KLOFE) & Institute of Advanced Materials (IAM), Jiangsu National Synergistic Innovation Center for Advanced Materials (SICAM), Nanjing Tech University (NanjingTech), 30 South Puzhu Road, Nanjing 211816, China.

[b]School of Chemical and Biomedical Engineering, Nanyang Technological University, 62 Nanyang Drive, Singapore 637459, Singapore.

E-mail: Liubin@ntu.edu.sg; iamxcdong@njtech.edu.cn

Table S1. Specific capacitance (F g^{-1}) at different current densities.

Samples	2 Ag^{-1}	4 Ag^{-1}	8 Ag^{-1}	10 Ag^{-1}	15 Ag^{-1}	20 Ag^{-1}	30 Ag^{-1}	40 Ag^{-1}	**Retention**
C@NM-300	633	582	520	487.5	446.25	405	352.5	320	**50.55%**
C@NM-500	1013	1000	886	865	776.25	695	645	550	**54.27%**
C@NM-700	1544	1500	1404	1388	1327	1280	1192	1170	**75.97%**
C@NM-900	1300	1270	1250	1220	1170	1121	1050.8	1005	**77.31%**

Note 1: "Retention" refers to the capacity at 40 A/g as compared with that at 2 A/g.

Table S2. Comparison of electrochemical performance of our C@Ni_3S_2@MoS_2 nanorods with the recently reported Ni_3S_2- and MoS_2-based hybrid materials

Materials	Capacitance (F/g)	Rate Performance	Capacitance retention	Reference
CNT@Ni_3S_2	514 (4 A/g)	70.4% (13.3/4)	88% (5.3A/g, 1500)	1
Ni_3S_2/rGO	1015.6 (1 A/g)	87.9% (10/1)	85% (10 A/g, 1000)	2
$NiCo_2O_4$@Ni_3S_2	1601 (2 A/g)	68.9% (20/2)	83.7% (4 A/g, 2000)	3
Ni@rGO− Ni_3S_2	987.8 (1.5 A/g)	54.3% (20/1.5)	97.9% (12 A/g, 3000)	4
ZnO@Ni_3S_2 array	1529 (2 A/g)	80.4% (20/2)	42% (10 A/g, 2000)	5
Ni3S2@$Ni(OH)_2$/3DGN	1037.5 (5.1 A/g)	38.4% (19.8/5.1)	99.1% (5.9 A/g, 2000)	6
Ni_3S_4@MoS_2	1440.9 (2 A/g)	55.56% (20/2)	90.7%(10 A/g, 3000)	7
C@Ni_3S_2@MoS_2	**1544 (2A/g)**	**82.9% (20/2)**	**92.8% (20 A/g, 2000)**	**Our work**

Note 2: "514 (4 A/g)" means the capacitance is 514 F/g at 4 A/g,

"70.4% (13.3/4)" refers to the capacitance at 13.3 A/g is 70.4% of that at 4 A/g,

"88% (5.3A/g, 1500)"represents that the capacitance retention is 88% after 1500 cycles at 5.3 A/g.

Table S3. Weight ratio of C, S, N and H from combustion analysis.

Samples	C (%)	S (%)	N (%)	H (%)
C@NM-300	11.01	14.03	5.14	2.09
C@NM-500	12.89	15.99	5.03	1.86
C@NM-700	16.72	13.22	5.00	1.52
C@NM-900	15.75	11.77	5.19	2.13

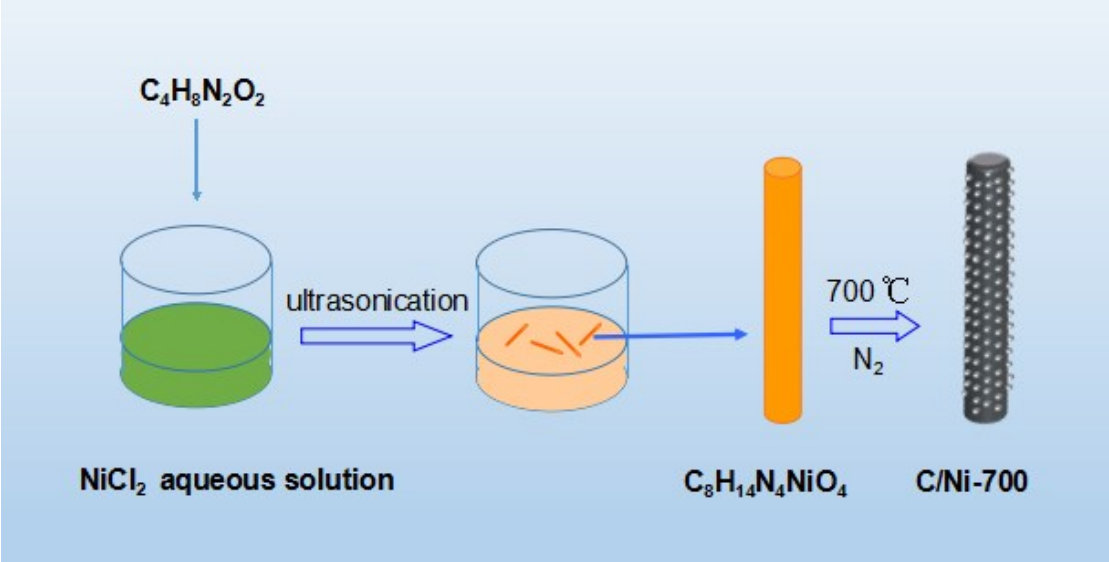

Fig. S1 Schematic illustration to show the formation of the C/Ni-700 nanorods.

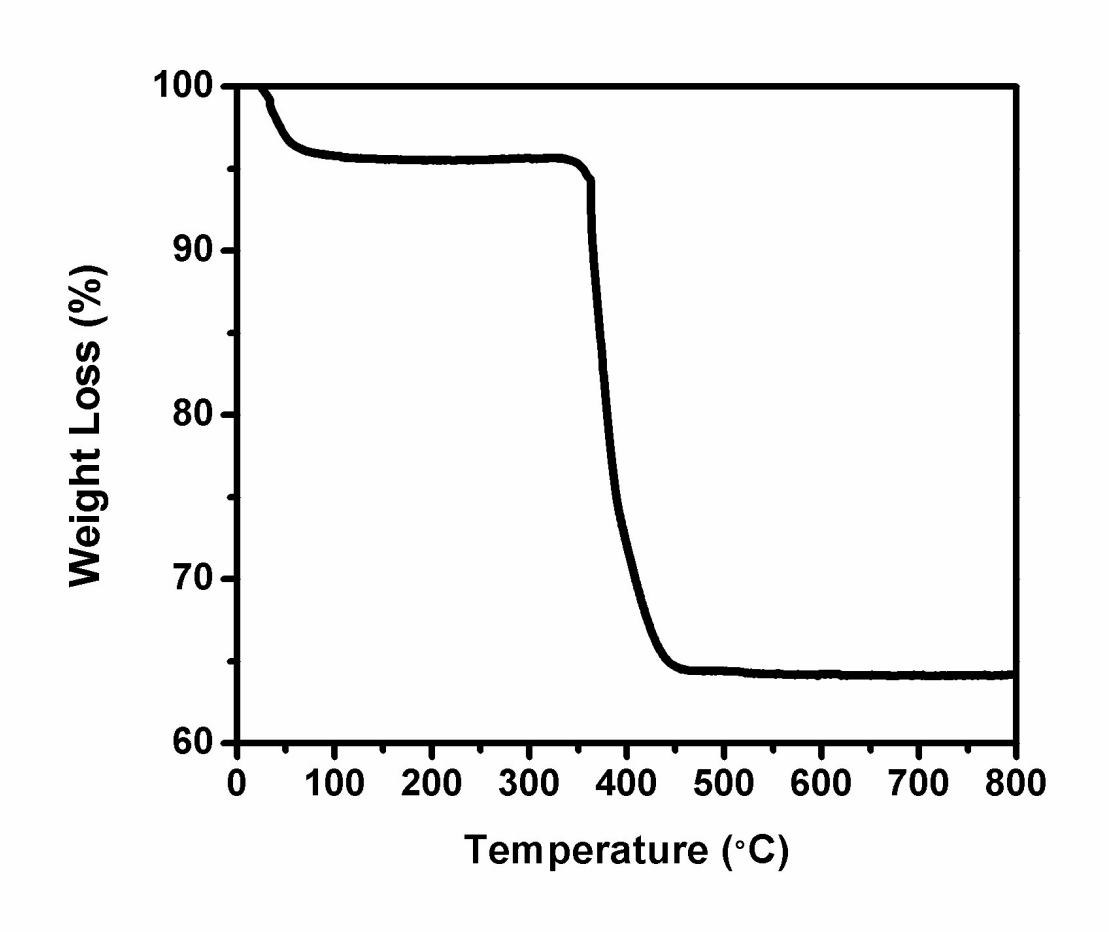

Fig. S2 Thermogravimetric curve of C/Ni-700 nanorods.

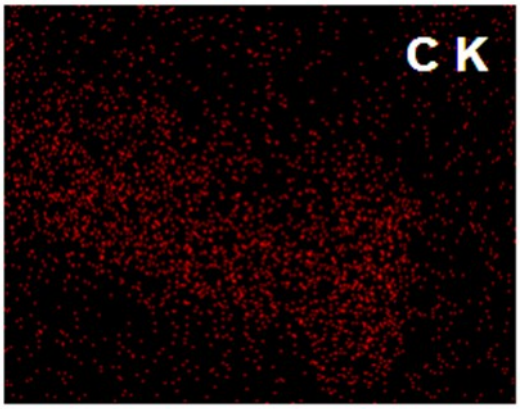

Fig. S3 EDX elemental mapping image for carbon.

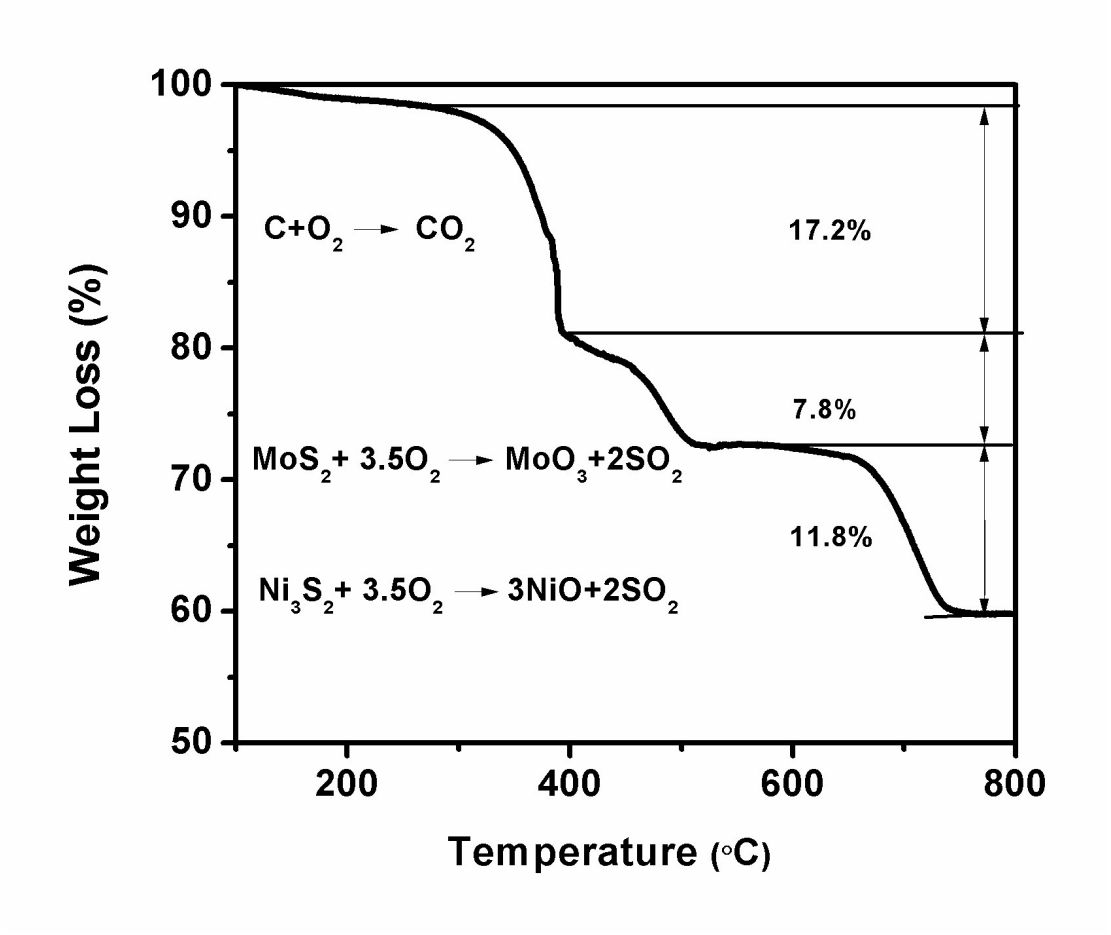

Fig. S4 Thermogravimetric curve of C@NM-700 double core-shell nanorods.

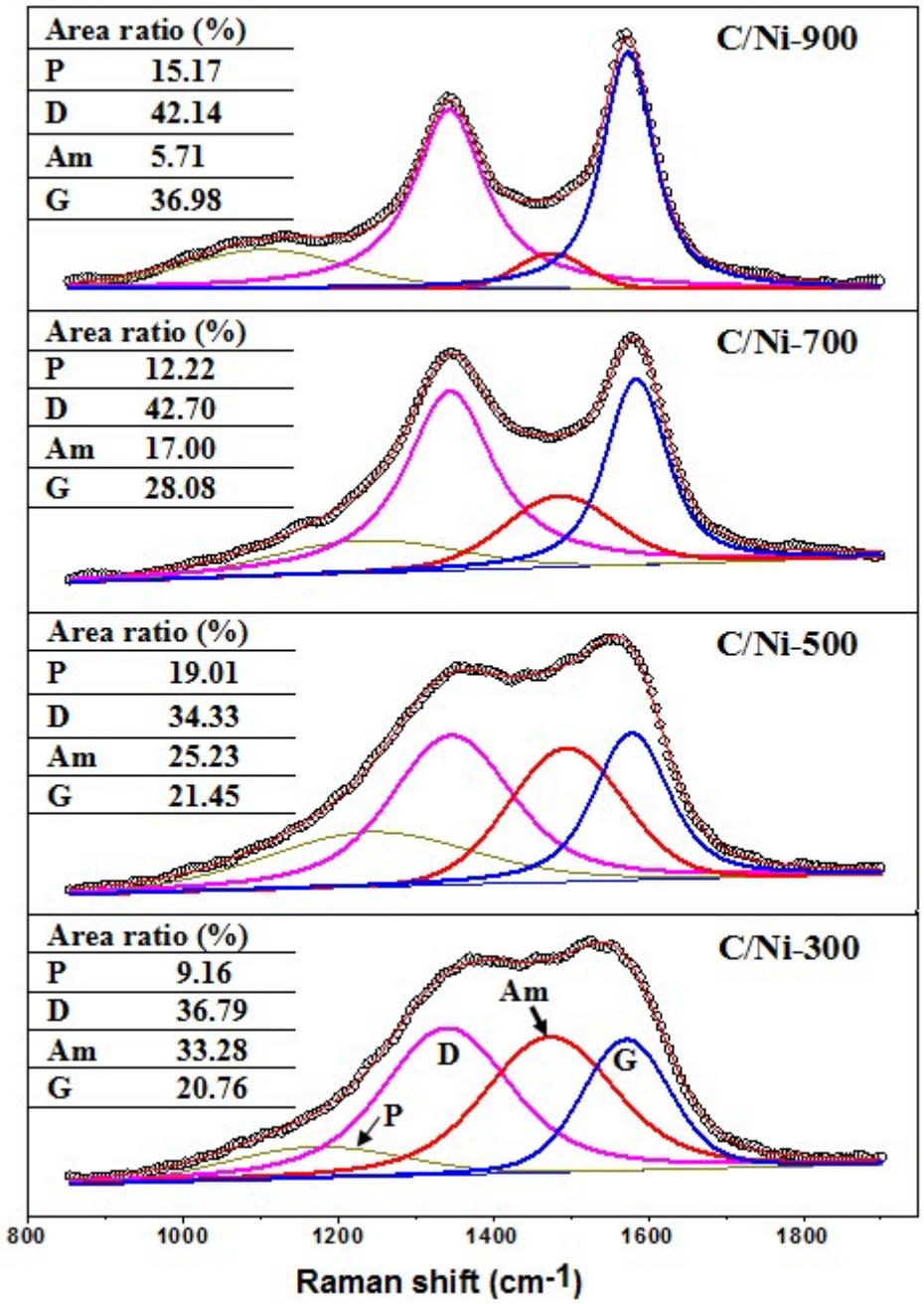

Fig. S5 Raman spectra of C/Ni-300, C/Ni-500, C/Ni-700, and C/Ni-900 nanorods. The insets show the ratio of (P) sp3, D (defect), Am (amorphous), G (graphite) carbon peaks.

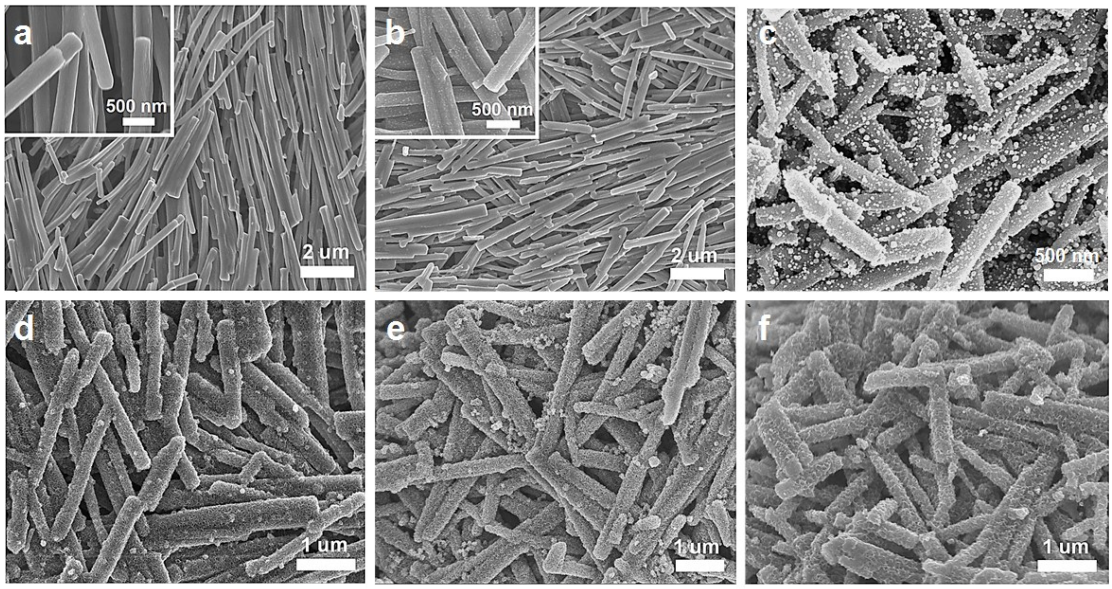

Fig. S6 (a & d) FESEM images of C/Ni-300 and C@NM-300 nanorods, (b & e) FESEM images of C/Ni-500 and C@NM-500 nanorods, (c & f) FESEM images of C/Ni-900 and C@NM-900 nanorods.

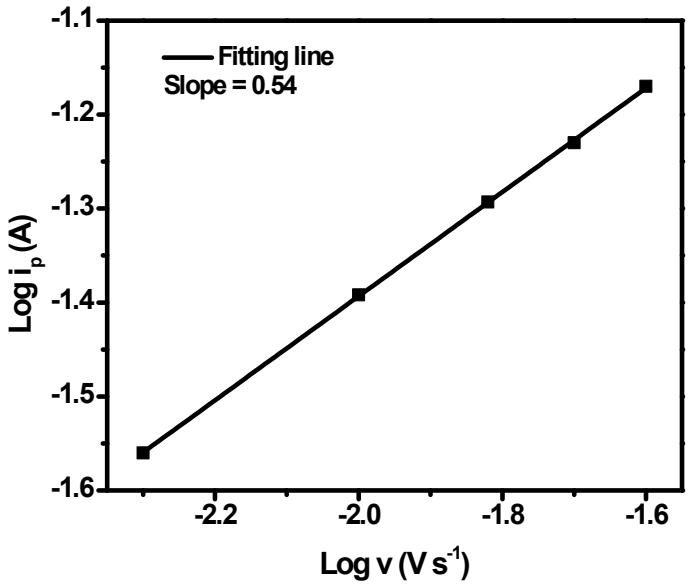

Fig. S7 Log(i_p) vs. log (v) plot, where i_p is the peak current and v is the scan rate, respectively.

Mode of reaction:

For diffusion-controlled reaction, the peak current (i_p) is proportional to the square root of the scan rate ($v^{1/2}$), derived from the Randles–Sevcik equation:[8]

$$i_p = 2.69 \times 10^5 n^{3/2} A D^{1/2} v^{1/2} C^* \quad \text{(S1)}$$

where i_p is the peak current (A), n is the number of transferred electrons, A is the area of the electrode (cm^2), D is the diffusion coefficient ($cm^2\ s^{-1}$), v is the scan rate ($V\ s^{-1}$) and C* is the bulk concentration of the analyte ($mol\ cm^{-3}$).

For adsorption-controlled reaction, i_p is directly proportional to v:[9]

$$i_p = (n^2 F^2 / 4RT) v A \Gamma^* \quad \text{(S2)}$$

where, i_p, n, v, and A have the same meaning as in Equation S1, F is the Faraday's constant, R is the gas constant ($J\ mol^{-1}\ K^{-1}$), and Γ* ($mol\ cm^{-2}$) is concentration of the analyte adsorbed on the surface of the electrode.

Accordingly, log(i_p) vs. log(v) was plotted in Fig. S7, which gave a slope of 0.54. As a result, it is concluded that the electrochemical reaction on C@Ni_3S_2@MoS_2 nanorods is mainly controlled by diffusion.

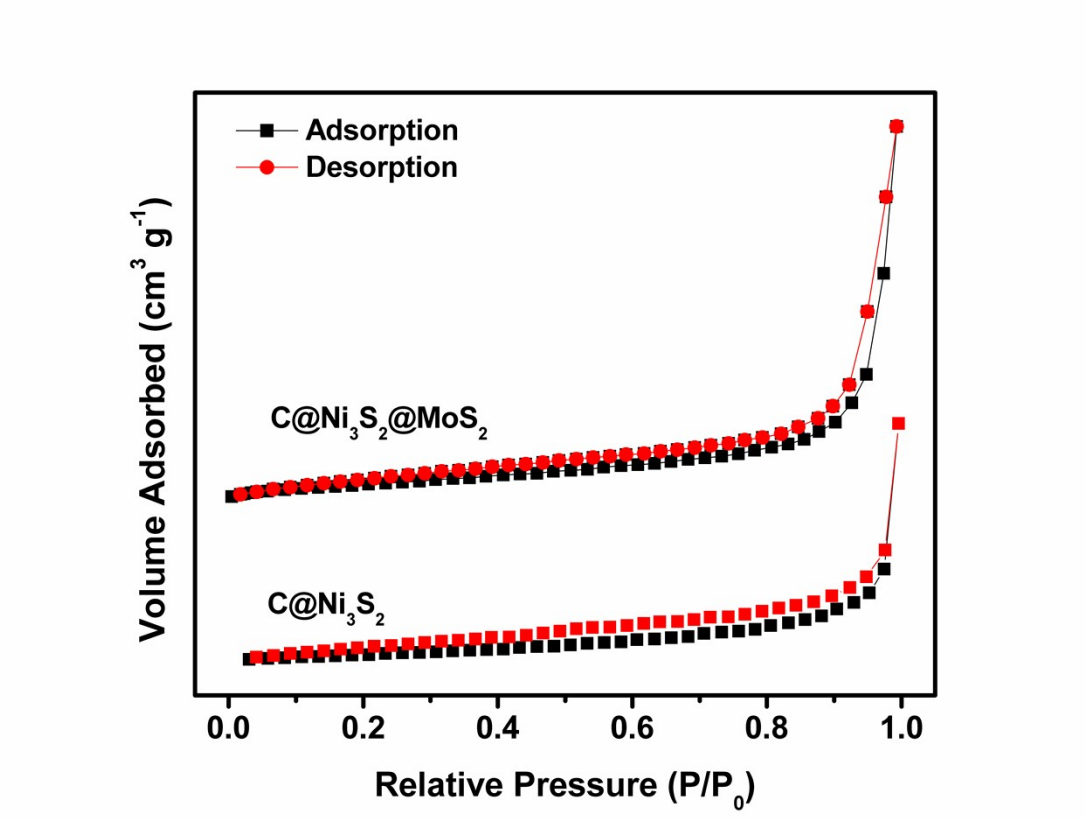

Fig. S8 Nitrogen adsorption-desorption isotherms of $C@Ni_3S_2$ and $C@Ni_3S_2@MoS_2$ nanorods.

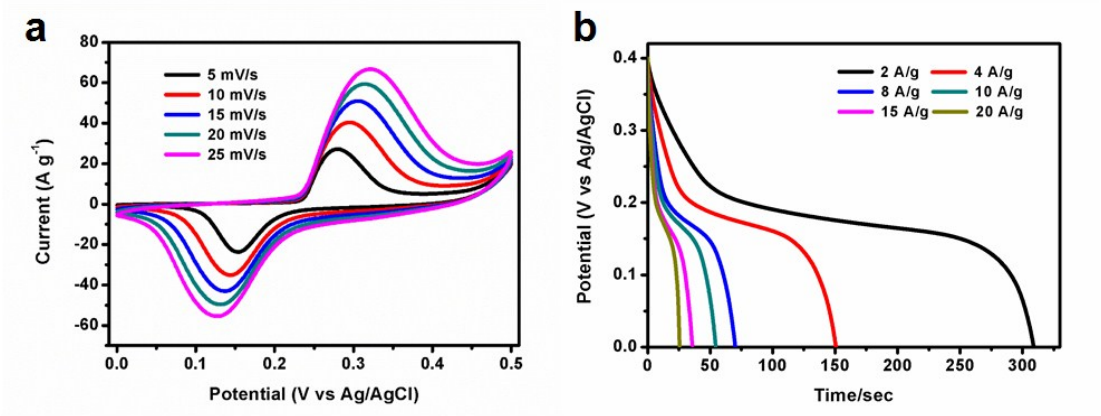

Fig. S9 (a) CV curves at different scan rates, and (b) discharge curves at different current densities for $C@Ni_3S_2@MoS_2$ nanorod electrode.

Detailed calculation of specific capacitance:

The specific capacitance can be calculated based on the following equation: $C = I \times \Delta t / (m \times \Delta V)$

where, I/m (A/g) is the specific current density, Δt (t) is the discharging time, ΔV (V) is the potential window for the charge-discharge process.

As shown in Fig. S9b, the discharging time of the C@Ni_3S_2@MoS_2 nanorod electrode at a current density of 2 A/g is 308.9 s, the potential window is 0.4 V, so the specific capacitance can be calculated as: 2×308.9/0.4 = 1544.5 F/g.

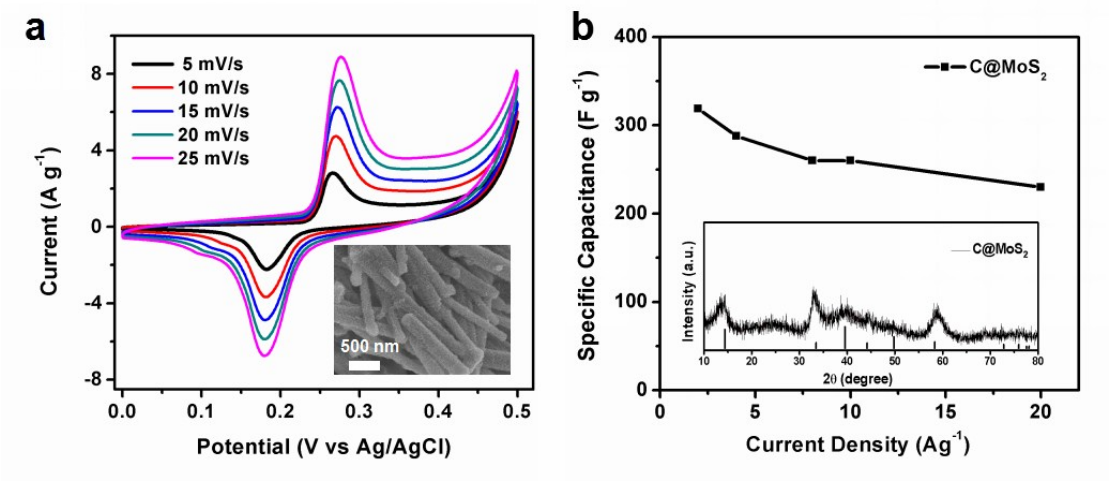

Fig. S10 (a) CV curves at different scan rates, and (b) specific capacitance obtained at different current densities for C@MoS_2 nanorods (the insets of (a) and (b) show SEM image and XRD pattern of C@MoS_2, respectively).

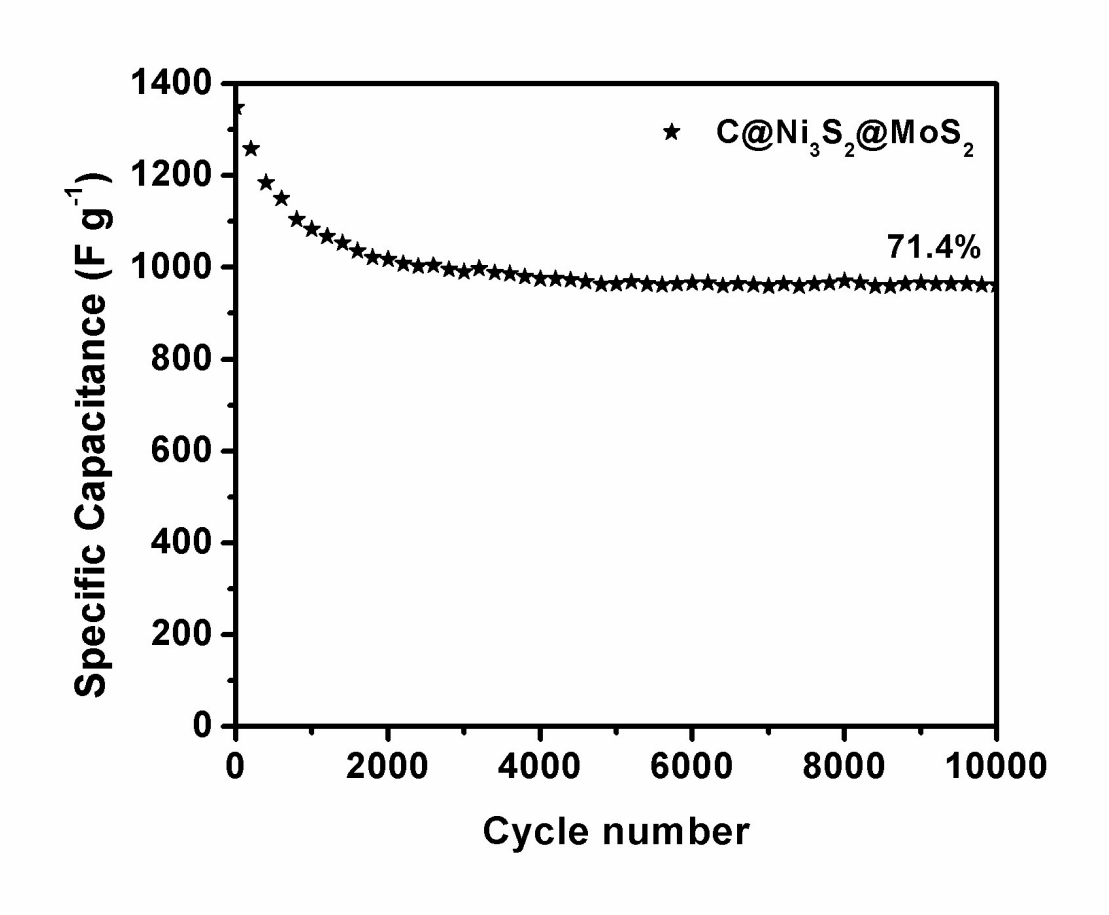

Fig. S11 Long-term cycling performance for the $C@Ni_3S_2@MoS_2$ nanorods at a current density of 10 A g^{-1}.

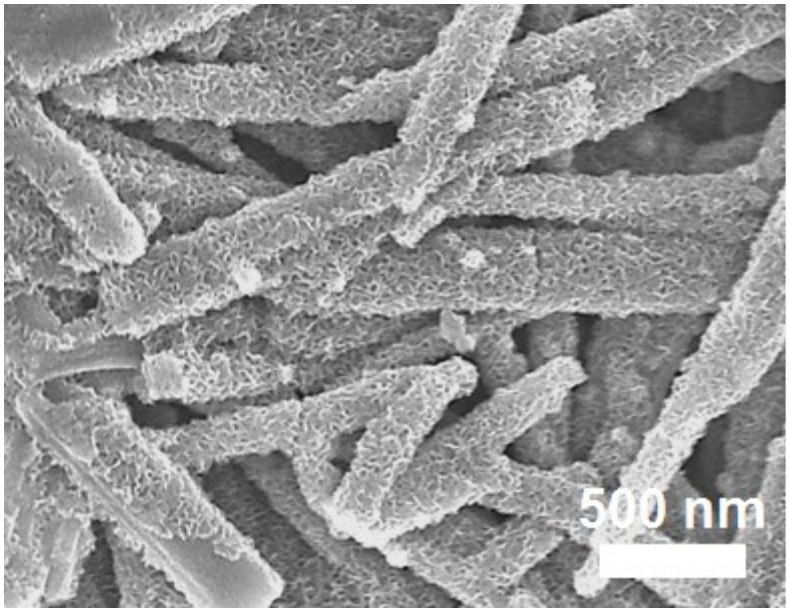

Fig. S12 SEM image of $C@Ni_3S_2@MoS_2$ after 2000 charging-discharging cycles at a current density of 20 A/g.

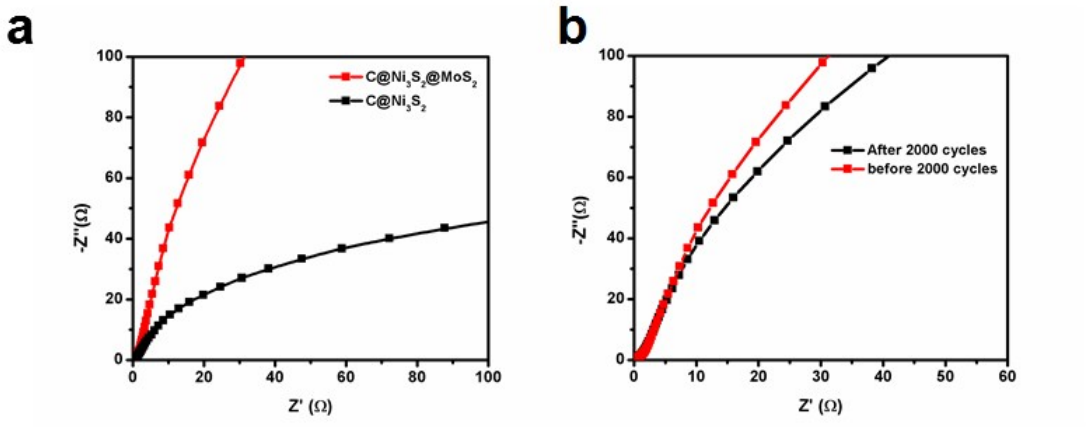

Fig. S13 (a) Nyquist plots of $C@Ni_3S_2$ and $C@Ni_3S_2@MoS_2$ nanorod electrodes, and (b) Nyquist plot of $C@Ni_3S_2@MoS_2$ nanorod electrode before and after 2000 charge-discharge cycles.

Supplementary Reference

1 T. Zhu, H. B. Wu, Y. B. Wang, R. Xu and X. W. Lou, *Adv. Energy Mater.,* 2012, **2**, 1497-1502.

2 X.W. Ou, L.Gan and Z. T. Luo, *J. Mater. Chem. A,* 2014, **2**, 19214-19220.

3 J. P. Wang, S.L. Wang, Z. C. Huang and Y. M. Yu, *J. Mater. Chem. A,* 2014, **2**, 17595-17601.

4 D. Ghosh and C. K. Das, *ACS Appl.Mater. Interfaces,* 2015, **7**, 1122−1131.

5 Z. C. Xing, Q. X. Chu, X. B. Ren, C. J. Ge, A. H. Qusti, A. M. Asiri, A. O. Al-Youbi and X. P. Sun, *J. Power Sources,* 2014, **245**, 17595-467.

6 W. J. Zhou, X. H. Cao, Z. Y. Zeng, W. H. Shi, Y. Y. Zhu, Q. Y. Yan, H. Liu, J. Y. Wang and H. Zhang, *Energy Environ. Sci.,* 2013, **6**, 2216-2221.

7 Y. Zhang, W. P. Sun, X. H. Rui, B. Li, H. T. Tan, G. L. Guo, S. Madhavi, Y. Zong and Q. Y. Yan, *Small*, 2014, **11**, 3694–3702.

8 B. Xu, M. L. Ye, Y. X. Yu and W. D. Zhang, Anal. *Chim. Acta*., 2010,**674**, 20-26.

9 L. A. Berben and J. C. Peters, *Chem. Commun*., 2010, **46**, 398-400.